Physica E: Low-dimensional Systems and Nanostructures 110 (2019) 1–4

Contents lists available at ScienceDirect

Physica E: Low-dimensional Systems and Nanostructures

journal homepage: www.elsevier.com/locate/physe

# Ultrafast rotation of CdS nanopods asserted from excited state dynamics

D.K. Swain, G. Mallik, S. Rath*

*School of Basic Sciences, Indian Institute of Technology Bhubaneswar, Arugul, Jatni, Khordha, Odisha, 752050, India*

ABSTRACT

The correlated optical and mechanical properties through fast dipolar interactions have been assessed from the excited state dynamics of the hexagonal phase cadmium sulphide nanopods (aspect ratio ~ 5.3) dispersion. The polarization dependent time resolved emission spectroscopy, and time dependent anisotropic analyses reveal the ultrafast rotation of the nanopods with time period 230.71 ns, and 559.03 ns along the parallel and perpendicular axis, respectively. This demonstrates the diligence of the nanopods as an excellent optically active rotor for nanomechanical systems.

Recent studies on the optically active nanoparticles dispersion have shown promising applications in energy harvesting [1], photothermal [2,3], photonics [4] and sensing [5]. Nevertheless, the influence of gyration in the photo-excited charge dynamics have kindled a great interest for practical applications of the anisotropic nanoparticle (e.g. nanorods (NRs) dispersion). For example, as per the dipole-electric field approximation ($\vec{\mu}\cdot\vec{E} \propto \cos^2\theta$, where $\vec{\mu}$ is the transition dipole, $\vec{E}$ is electric field component, and $\theta$ is the angle between $\vec{\mu}$ and $\vec{E}$), the orientation between the photo-excited dipoles, and emitted dipoles may change due to the rotation of the dispersed NRs under the influence of electromagnetic field [6] within the time-frame of lifetime of the dipole. As a consequence, there will be a fluctuation in the excited states orientation yielding the modulation in the emission intensity [7,8]. In analogy, the excited states of the NRs, where the carrier exhibits longitudinal and transverse modes of localization, acquit anisotropic emission depending upon the orientation of the crystal [9–12]. Thus, the optical properties of the NRs dispersed in a fluid, where they experience gyration under an external electromagnetic field [13], is an important point of debate for application in the nanomechanical devices [14]. For instance, though the optical torque [15], optical vertex [16], and Brownian force [17] activated rotation in the low frequency range are reported in the field of nanomotor, the ultrafast rotational properties of nanorods, and its derived structures viz. nanopods, are less understood so far. Inspired by its formidable phenomena and applications, and to observe the rotational effect through the excited state dynamics, we have synthesized high quality cadmium sulphide (CdS) nanopods (two or more nanorods join together at a common end) as a color emitter upon photo-excitation using the chemical based growth technique. The optical properties of the nanopods (NPDs), dispersed in a fluid (e.g. chloroform), have been studied using optical absorption and emission measurements. The excited state dynamics of the NPDs dispersion have been studied using polarization dependent time resolved emission spectroscopy (PTRES) and time dependent anisotropic (TDA) measurements, indicating the rotation of the CdS NPDs in the nanosecond time period.

In a typical synthesis, 0.063 g of cadmium chloride ($CdCl_2$) salt was added to the 1:1 mixture of octylamine and oleylamine solvent. The solution was heated at 393 K, for 2 h to functionalize the cadmium (Cd). Subsequently, the Cd-functionalised powders were collected using a precipitation technique in the presence of hexane followed by centrifugation. Separately, sulfur (S) solution was prepared by dissolving 0.058 g of sulfur powder in a solvent containing 1:1 mixture of octylamine and oleylamine. Then, the Cd-functionalised powder was added to the S-solution under vigorous stirring condition for 20 min. Finally, the resultant solution was autoclaved at 373 K for 24 h. The CdS nanorod powders were collected by washing it with an excess of tri-n-octylphosphine oxide solution and ethanol, successively. The extracted CdS nanorod powders were dispersed in the chloroform for the PTRES and TDA measurements.

The morphology of the sample collected on a carbon coated copper grid has been studied using transmission electron microscope (TEM). Fig. 1 (a) shows the TEM micrograph of the sample. As observed from the TEM, the sample exhibits a distribution of nanorods joined at a common end forming nanopod structures (e.g., bipods and tripods). The average length, diameter, and aspect ratio (length/diameter) of the arms of the NPDs were calculated as 37.20 nm, 7.50 nm and 5.30, respectively. Fig. 1 (c) shows the distribution of aspect ratio of one hundred selected NPD image. The high resolution TEM image of a single arm of the CdS NPD, shown in Fig. 1 (b), revealed the lattice distance as 0.34 nm confirming the hexagonal structure of the sample. Further, the crystallinity of the sample has been studied using the wide angle X-ray scattering (WAXS) measurements. Fig. 1 (d) shows the WAXS pattern of the sample. The crystallographic planes (100), (002),

* Corresponding author.
*E-mail address:* srath@iitbbs.ac.in (S. Rath).

https://doi.org/10.1016/j.physe.2019.01.026
Received 27 December 2018; Accepted 26 January 2019
Available online 31 January 2019
1386-9477/ 

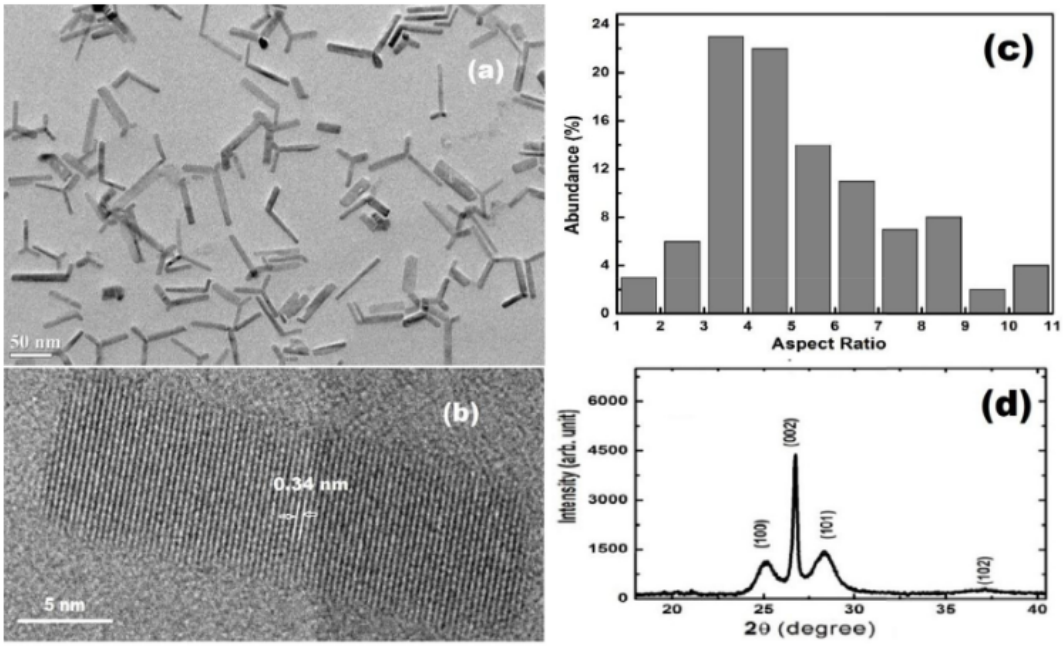


**Fig. 1.** (a) The TEM micrograph of the CdS NPDs, (b) the HRTEM image of an arm of the NPD, (c) Bar diagram representing the distribution of the aspect ratio of the NPD and (d) the WAXS patterns of the CdS NPDs.

and (101) correspond to hexagonal structure of the CdS as per the (JCPDS#80-006) standard data. It is to be noted that the peak related to the plane (002) is narrow and intense compared to other peaks, which is due to the extended growth along the c-axis of the NRs. Using the Debye Scherrer's formula, $D = \frac{0.94 \times \lambda}{\beta \cos \theta}$, the length and diameter has been calculated to be 31.93 nm and 5.72 nm from the full width at half maxima ($\beta$) of the peak corresponding to the planes, (002) and (101), respectively, giving an aspect ratio of 5.50.

The optical properties of the CdS NPDs dispersion have been studied using the Perkin Elmer UV–Vis Spectrophotometer, and the Horiba Scientific FluroMax-4 Spectrofluorometer. The absorption (left arrow) and emission spectra (right arrow) are shown in Fig. 2 (a). The spectrum shows a strong absorption onset at wavelength, 500 nm. The confined band gap of the CdS NPDs has been estimated to be 2.48 eV using the relation [18], $\alpha = A(h\nu - E_g)^{1/2}$, where $\alpha$, $\nu$ and $E_g$ are the absorbance, the frequency of the excitation source, and bulk band gap (2.42 eV), respectively. The observed blue shift of 0.06 eV corresponds to the exciton energy. According to the even mirror boundary condition (EMBC) model [19] in a weak confinement regime for the cylindrical nanostructure, the excitonic ground state energy, $E_{GS}$, can be expressed as, $E_{GS} = \frac{h^2}{2\mu}\left(\frac{0.268}{a^2} + \frac{1}{4c^2}\right)$, where, $a$, $c$, and μ are the diameter, length and reduced mass of the exciton, respectively. Taking $a$ as 7.50 nm and $c$ as 37.20 nm from the TEM studies and reduced mass, $\mu_{CdS} = 0.166m_0$, $E_{GS}$ is calculated to be 0.045 eV. Interestingly, the observed value of $E_{GS}$ from the experiment is in agreement with the EMBC model. Furthermore, the emission spectrum of the CdS NPDs for excitation wavelength, 375 nm, gives a distinct narrow peak at wavelength, 514 nm corresponding to the band edge emission. In comparison to the optical

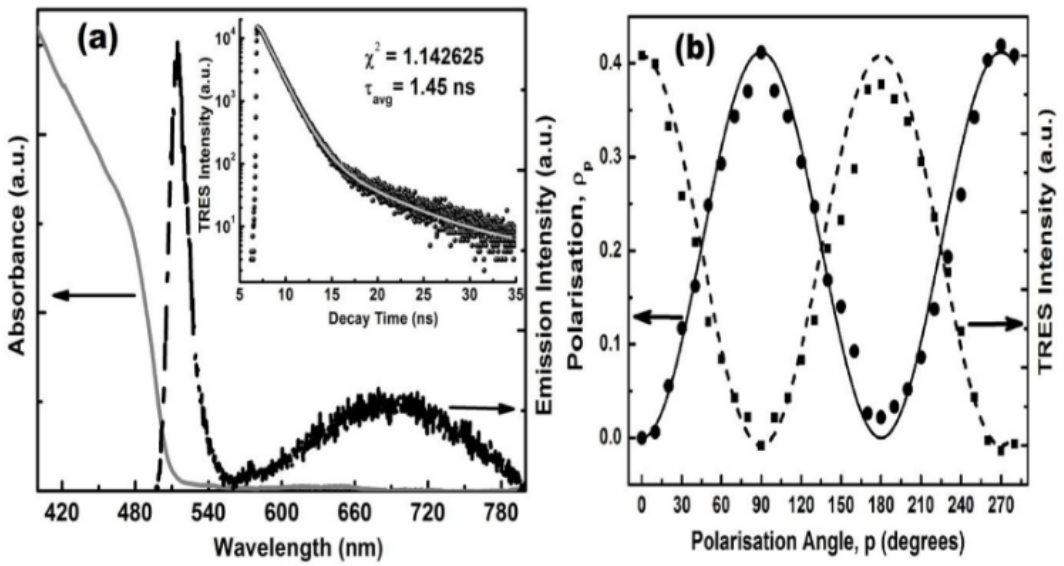


**Fig. 2.** (a) Absorption and Emission spectra of the CdS NPDs dispersed in the chloroform. Inset is the Time-resolved emission decay plot and gray line is a double exponential fitting curve. (b) The plot of the degree of polarization (filled circle) and the TRES intensity (filled box) at emission line 514 nm as a function of the polarization angle. The dotted line indicates a $\cos^2 \theta$ fit showing the linear polarization of the emission properties.

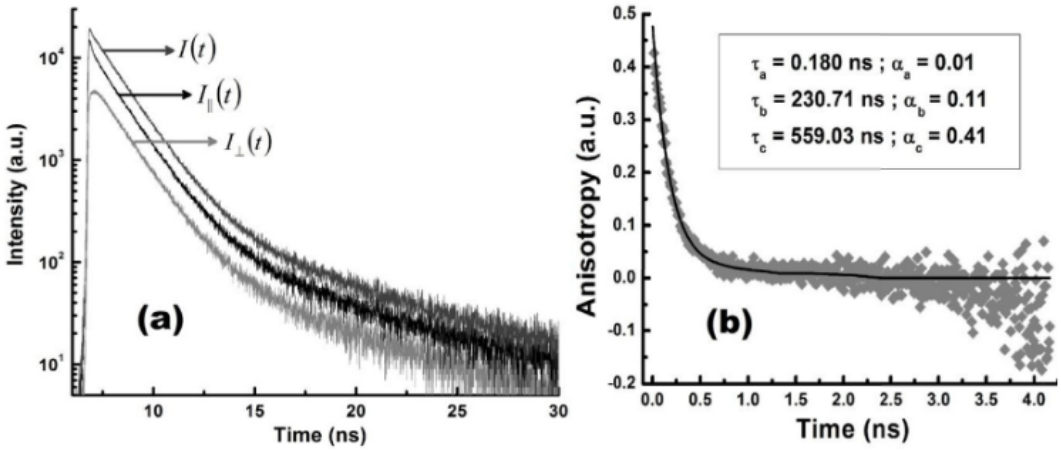


**Fig. 3.** (a) The PTRES decay profiles of the NPDs at emission line 514 nm in parallel ($I_{\parallel}(t)$) and perpendicular ($I_{\perp}(t)$) polarization configuration. $I(t)$ is the integral decay intensity. (b) The TDA spectrum (gray diamonds) of the sample dispersed in the chloroform. From the triple exponential decay fit (black line), the $\tau_a$, $\tau_b$, $\tau_c$ are estimated to be 0.180 ns, 230.71 ns and 559.03 ns respectively.

absorption, the emission spectrum shows a Stokes shift of 67.5 meV related to the interaction of the exciton with the medium. The broad emission peak at wavelength, 700 nm is probably due to the transitions from the defect/surface states [20].

The photo-excited state dynamics of the CdS NPDs have been studied from the PTRES and the TDA measurements using Horiba Time-correlated Single Photon Counting (TCSPC) set up in the presence of a pulsed diode laser (wavelength ~ 375 nm, pulse rate ~ 1 MHz and pulse width ~ 200 ps). The time resolved emission spectrum (TRES) at emission line, 514 nm under pulsed laser beam excitation, is shown as an inset in Fig. 2 (a). From the double exponential decay fitting, the amplitudes ($\alpha_i$) and time periods ($\tau_i$) of the transitions are estimated as $\alpha_1 = 10.25$, $\tau_1 = 1.30$ ns and, $\alpha_2 = 0.36$, $\tau_2 = 6.97$ ns, respectively; yielding the average life time of the exciton [21], $\langle\tau\rangle = \frac{\alpha_1\tau_1^2 + \alpha_2\tau_2^2}{\alpha_1\tau_1 + \alpha_2\tau_2}$ as 1.45 ns. The transition dipole moment, $|\mu| = \left(\frac{3\pi\hbar c^3\varepsilon_0}{\omega^3\tau}\right)^{\frac{1}{2}}$ corresponding to the excited state has been estimated as 17.26 $D$ (Debye). In order to understand the effect of electromagnetic field induced rotation, the TRES studies have been carried out at a different polarization angle. The degree of polarization, $\rho_p$ at a given polarization angle has been evaluated using the relation [9,21], $\rho_p = \frac{I_{\parallel} - I_p}{I_{\parallel} + I_p}$, where $I_{\parallel}$ is the TRES intensity with analyzer angle same as that of the polarizer (parallel configuration), and $I_p$ is the TRES intensity at analyzer angle '$p$' degree with respect to the polarizer. Fig. 2 (b) shows the variation of $\rho_p$ (indicated by left arrow), and TRES intensity (indicated by right arrow) as a function of polarization angle. The dotted line indicates a $\cos^2\theta$ fit to the TRES intensities showing a linearly polarized behavior of excited states in the NPDs [22]. The value of $\rho_{max}$ is calculated to be 0.42 for $p = 90$ degrees (perpendicular configuration). A similar degree of polarization ($\rho < 0.6$) has been observed by Wang et al. [9] for 1-D nanostructures. The decay period, and transition dipole moment corresponding to the parallel and perpendicular polarization configuration has been estimated to be $\tau_{\parallel} = 1.52ns$, $|\mu_{\parallel}| = 16.88D$, and $\tau_{\perp} = 1.61ns$, $|\mu_{\perp}| = 16.40D$, respectively. This affirms a change in the net transition dipole moment of 3% possibly due to the rotation dependent alignment of the NPDs.

Further, the influence of shape anisotropy on the dynamics of the excited state has been investigated using the TDA measurements. The integral decay intensity [21] $I(t) = I_{\parallel}(t) + 2I_{\perp}(t)$, and the anisotropic decay, $r(t) = \frac{I_{\parallel}(t) - I_{\perp}(t)}{I(t)}$ are shown in Fig. 3 (a) & (b), respectively, where $I_{\parallel}(t)$ and $I_{\perp}(t)$ are the intensity for parallel and perpendicular polarization. It is to be noted that, in case of the anisotropic fluorophore dispersion, the uncorrelated emission lifetimes and rotational correlation times are related through the anisotropic decay [23], $r(t) = \alpha_a e^{\frac{-t}{\tau_a}} + \alpha_b e^{\frac{-t}{\tau_b}} + \alpha_c e^{\frac{-t}{\tau_c}}$, where the time coefficients, $\tau_a$, $\tau_b$, $\tau_c$ correspond to the time period of the segmental motion, rotation around the parallel axis and perpendicular axis, respectively. From the triple exponential decay fitting of Fig. 3 (b), represented by a black line, the values of$\tau_a$, $\tau_b$ and $\tau_c$ are estimated to be 0.180 ns, 230.71 ns and 559.03 ns with corresponding fundamental anisotropy, $\alpha_a = 0.01$, $\alpha_b = 0.11$ and $\alpha_c = 0.41$, respectively. Additionally, as per the Perrin's expression [23,24], the rotational time period, $\tau_c = \frac{4\pi R_g^3\eta}{3k_BT}$, where hydrodynamic radius of gyration [23], $R_g = \sqrt{\frac{L^2}{12} + \frac{d^2}{8}}$ is a function of length, L and diameter, d of the nanorods. $k_B$, $\eta$ and $T$ are the Boltzmann constant, viscosity of the medium and temperature, respectively. Considering the viscosity, $\eta = 0.563$ mPa s of chloroform (medium), $T = 300$ K and $\tau_c = 559.03$ ns, the value of $R_g$ for the NPDs is calculated to be 9.86 nm, which corresponds to the NRs having average length and diameter of 32.2 nm and 5.70 nm, respectively. The results are consistent with the average size obtained from the TEM, WAXS and TDA studies within experimental limitations.

In summary, the CdS nanopods with aspect ratio of 5.30 have been synthesized using a micellar based growth technique. The optical properties of the NPD dispersed in a fluid (chloroform) has been analyzed under pulsed laser excitation, shows an anisotropy in the excited state dynamics with the degree of polarization as 42% which is corresponding to a change in the orientation of the excitonic dipole. This suggests a co-related opto-mechanical behaviors of the NPD in a viscous fluid. As observed from the TDA analysis, the effective rotational time period is found to be longer along the perpendicular axis of rotation (559.03 ns) in comparison to the parallel axis of rotation (230.71 ns). This investigation sheds light on the possible application of the CdS NPD as an efficient dipole-dipole interaction guided nano-rotors.

## Acknowledgement

S. R. acknowledges Dr. B. Satpati, SINP Kolkata and Mr. A. Pradhani, IIT BBS for the help received during TEM studies and sample preparations.

## Appendix A. Supplementary data

Supplementary data to this article can be found online at https://doi.org/10.1016/j.physe.2019.01.026.

## References

[1] D. Erickson, D. Sinton, D. Psaltis, Optofluidics for energy applications, Nat. Photon.

5 (2011) 583–590, https://doi.org/10.1038/nphoton.2011.209.
[2] C.H. Chou, C.D. Chen, C.R.C. Wang, Highly efficient, wavelength-tunable, gold nanoparticle based optothermal nanoconvertors, J. Phys. Chem. B 109 (2005) 11135–11138, https://doi.org/10.1021/jp0444520.
[3] G.L. Liu, J. Kim, Y.U. Lu, L.P. Lee, Optofluidic control using photothermal nanoparticles, Nat. Mater. 5 (2006) 27–32, https://doi.org/10.1038/nmat1528.
[4] K.S. Lee, S.Y. Yoon, K.H. Lee, S.B. Kim, H.J. Sung, S.S. Kim, Optofluidic particle manipulation in a liquid-core/liquid-cladding waveguide, Optic Express 20 (2012) 17348, https://doi.org/10.1364/OE.20.017348.
[5] X. Fan, I.M. White, S.I. Shopova, H. Zhu, J.D. Suter, Y. Sun, Sensitive optical biosensors for unlabeled targets: a review, Anal. Chim. Acta 620 (2008) 8–26, https://doi.org/10.1016/j.aca.2008.05.022.
[6] T.B. Jones, Electromechanics of Particles, Cambridge University Press, New York, 2005.
[7] M. Ehrenberg, R. Rigler, Rotational brownian motion and fluorescence intensify fluctuations, Chem. Phys. 4 (1974) 390–401, https://doi.org/10.1016/0301-0104(74)85005-6.
[8] J.E.T. Corrie, J.S. Craik, V.R.N. Munasinghe, A homobifunctional rhodamine for labeling proteins with defined orientations of a fluorophore, Bioconjug. Chem. 9 (1998) 160–167, https://doi.org/10.1021/bc970174e.
[9] J. Wang, M.S. Gudiksen, X. Duan, Y. Cui, C.M. Lieber, Highly polarized photoluminescence and photodetection from single indium phosphide nanowires, Science 293 (80) (2001) 1455–1457, https://doi.org/10.1126/science.1062340.
[10] R. Agarwal, C.J. Barrelet, C.M. Lieber, Lasing in single cadmium sulfide nanowire optical cavities, Nano Lett. 5 (2005) 917–920, https://doi.org/10.1021/nl050440u.
[11] X. Zhang, J. Qin, Y. Xue, P. Yu, B. Zhang, L. Wang, R. Liu, Effect of aspect ratio and surface defects on the photocatalytic activity of ZnO nanorods, Sci. Rep. 4 (2014) 4596, https://doi.org/10.1038/srep04596.
[12] Y.J. Doh, K.N. Maher, L. Ouyang, C.L. Yu, H. Park, J. Park, Electrically driven light emission from individual CdSe nanowires, Nano Lett. 8 (2008) 4552–4556, https://doi.org/10.1021/nl802797y.
[13] Y.-K. Kim, B. Senyuk, O.D. Lavrentovich, Molecular reorientation of a nematic liquid crystal by thermal expansion, Nat. Commun. 3 (2012) 1133, https://doi.org/10.1038/ncomms2073.
[14] J.M. Tsay, S. Doose, S. Weiss, Rotational and translational diffusion of peptide-coated CdSe/CdS/ZnS nanorods studied by fluorescence correlation spectroscopy, J. Am. Chem. Soc. 128 (2006) 1639–1647, https://doi.org/10.1021/ja056162i.
[15] A. Lehmuskero, R. Ogier, T. Gschneidtner, P. Johansson, M. Käll, Ultrafast spinning of gold nanoparticles in water using circularly polarized light, Nano Lett. 13 (2013) 3129–3134, https://doi.org/10.1021/nl4010817.
[16] Z. Yan, N.F. Scherer, Optical vortex induced rotation of silver nanowires, J. Phys. Chem. Lett. 4 (2013) 2937–2942, https://doi.org/10.1021/jz401381e.
[17] T.C. Lee, M. Alarcón-Correa, C. Miksch, K. Hahn, J.G. Gibbs, P. Fischer, Self-propelling nanomotors in the presence of strong Brownian forces, Nano Lett. 14 (2014) 2407–2412, https://doi.org/10.1021/nl500068n.
[18] J.I. Pankove, Optical Processes in Semiconductor, Dover Publication Inc, New York, 1971.
[19] Y. V Vorobiev, B. Mera, V.R. Vieira, P.P. Horley, J. González-Hernández, Weak and strong confinements in prismatic and cylindrical nanostructures, Nanoscale Res. Lett. 7 (2012) 371, https://doi.org/10.1186/1556-276X-7-371.
[20] J.R. Lakowicz, I. Gryczynski, Z. Gryczynski, K. Nowaczyk, C.J. Murphy, Time-resolved spectral observations of cadmium-enriched cadmium sulfide nanoparticles and the effects of DNA oligomer binding, Anal. Biochem. 280 (2000) 128–136, https://doi.org/10.1006/abio.2000.4495.
[21] M. Ameloot, M. vandeVen, A.U. Acuña, B. Valeur, Fluorescence anisotropy measurements in solution: methods and reference materials (IUPAC Technical Report), Pure Appl. Chem. 85 (2013) 589–608, https://doi.org/10.1351/PAC-REP-11-11-12.
[22] D.V. Talapin, R. Koeppe, S. Götzinger, A. Kornowski, J.M. Lupton, A.L. Rogach, O. Benson, J. Feldmann, H. Weller, Highly emissive colloidal CdSe/CdS heterostructures of mixed dimensionality, Nano Lett. 3 (2003) 1677–1681, https://doi.org/10.1021/nl034815s.
[23] H.Y. Weng, K.M. Lee, Y.S. Chen, C.W. Chang, Conformational dynamics and excitation wavelength dependent photoluminescence of decameric organic nanoparticles, Phys. Chem. Chem. Phys. 15 (2013) 16935–16940, https://doi.org/10.1039/c3cp52137k.
[24] A. Ortega, J. García de la Torre, Hydrodynamic properties of rodlike and disklike particles in dilute solution, J. Chem. Phys. 119 (2003) 9914–9919, https://doi.org/10.1063/1.1615967.